Available online at www.sciencedirect.com
SCIENCE DIRECT
ELSEVIER
Journal of the European Ceramic Society 26 (2006) 849–859
ECERS
www.elsevier.com/locate/jeurceramsoc

Combinatorial hydrothermal synthesis and characterisation of perovskites

R. Wendelbo *, D.E. Akporiaye, A. Karlsson, M. Plassen, A. Olafsen

SINTEF Materials and Chemistry, P.O. Box 124, Blindern, N-0314, Norway

Received 1 October 2004; received in revised form 18 December 2004; accepted 27 December 2004
Available online 8 April 2005

Abstract

In the present work we have applied combinatorial methodology to the hydrothermal synthesis and characterisation of perovskites. In a first series with 48 samples in the (Pb,Ba,Sr)ZrO_3 compositional field, synthesis conditions were optimised by variation of pH. In a second series of 96 samples the (Pb,Ba)(Zr,Ti)O_3 compositional field was investigated, with the aim to control crystallinity and particle size. Using powder X-ray diffraction (XRD), it was established that most compositions crystallised readily within 3–23 h at 200 °C in 2.0–3.3 M KOH. Using scanning electron microscopy (SEM), particle size was determined to be from 3 to 8 μm for the pure zirconates to 0.2–1 μm for the pure titanates. Microprobe wavelength dispersive spectroscopy (WDS) was used for chemical analysis. It was found that particle size was determined primarily by bulk chemistry whereas a polyacrylamide additive and pH had little effect. It has been shown that combinatorial hydrothermal synthesis and characterisation techniques are fully applicable to the synthesis and basic characterisation of perovskites.

Keywords: Perovskites; Combinatorial; Powders-chemical preparation; Grain size; Hydrothermal methods

1. Introduction

Combinatorial methods are well-suited for preliminary screening of multi-parameter spaces, typically where complex compositions are desired. Briceno et al.[1] synthesised arrays of oxides, including perovskites using combinatorial thin film deposition and physical masking techniques, and Reichenbach and McGinn[2] synthesised arrays of perovskites applying a polymerisable complex method. At SINTEF, combinatorial hydrothermal techniques were originally developed for the synthesis of zeolites.[3] The system built around our *MultiAutoclave*[4] has been extended and refined to various applications within the field of catalysis.[5–6]

Perovskite and materials with a perovskite-like structure can be described by the general formula ABO_3. In the following, these materials will be referred to as perovskites. Many perovskites have useful electronic properties. Among these are lead zirconate titanate (PZT) which is a piezoelectric material of commercial importance,[7–8] and barium titanate (BT) which has useful dielectric and ferroelectric properties.[9]

Perovskites can be prepared by a variety of methods such as the much used sol–gel-, complexation- (e.g. citric acid), hydrothermal-, and conventional ceramic synthesis methods. The advantages of hydrothermal synthesis as compared to other methods are that fine powders with tuneable particle size and uniform morphology with good sintering properties, low contamination by impurities and controlled agglomeration can be obtained.[7–12] For example, within the family of perovskites formed with Ba, Sr and Pb as A-ion and Ti and Zr as B-ions hydrothermal synthesis of perovskites have been reported for $BaTiO_3$,[13–17] $PbTiO_3$,[10,18,19] $SrZrO_3$,[14] and the solid solution series $PbZr_xTi_{1-x}O_3$,[7,8,20–25] $BaZr_xTi_{1-x}O_3$[11] and $Pb_xBa_{1-x}TiO_3$.[9]

Important parameters in hydrothermal synthesis of perovskites are pH, reaction time, temperature and the presence of additives. pH must be within a certain range for certain phases or compositions to form, and will also often affect particle size.[7,10] The presence of salts may hamper the substitution of elements into the structure, and may hinder complete crystallisation.[7]

In combinatorial preliminary screenings, the ambition is to rapidly obtain indications to promising candidates for

* Corresponding author. Tel.: +47 98 243 940; fax: +47 22 067 350.

0955-2219/$ – see front matter © 2005 Elsevier Ltd. All rights reserved.
doi:10.1016/j.jeurceramsoc.2004.12.031

further focused work. The aim of the present work has primarily been to implement our combinatorial techniques to the hydrothermal synthesis of a broad range of perovskites, and to demonstrate the breadth of information that can be extracted from combinatorial basic characterisation. We have chosen to target perovskites with Pb, Ba and Sr as A-ions and Zr and Ti as B-ions. A further aim has been to manipulate the particle size of the products.

2. Experimental

2.1. Hydrothermal synthesis

The hydrothermal synthesis procedures was based on our combinatorial approach[3,4] which has now been based on a standardised format. Forty-eight syntheses are carried out in parallel using Teflon sample holders having volumes of about 2 ml. In-house developed software[26] based on LabVIEW is used to control instrumentation, and to monitor and log all relevant data during the entire process. Synthesis parameters such as reagents, temperature, synthesis time, pH and additives were chosen with basis primarily in the works of Sato et al.[10] and Vivekanandan et al.[11] with the aim to verify our methodology with reference to their results.

1.5 M aqueous solutions of $TiOCl_2$ and $ZrOCl_2$ were prepared from $TiCl_4$ (Aldrich) and $ZrOCl_2$ (Fluka, ≥99%). The $TiOCl_2$ was freshly prepared. 1.0 M solutions of Pb, Ba, and Sr were prepared from $BaCl_2$ (Aldrich, 99%), $Pb(NO_3)_2$ (Aldrich, 99+%) and $Sr(NO_3)_2$ (Merck, p.a.). KOH (Merck, p.a.) was used as a 10 M solution and Polyacrylamide (PAAm) with molecular weight of about 10,000 (Aldrich, 50% aqueous solution) diluted to 0.9 wt.% was used. The various reagents were added in the form of liquid solutions by means of a Zinsser Lissy pipetting robot, while the mixtures were simultaneously shaken. Good mixing was aided by presence of steel beads in the mixtures. Mixtures were transferred to the MultiAutoclave,[4] which was heat treated under autogeneous pressures at 200 °C.

In a first experimental series (series 1), eight different combinations of Pb, Ba and Sr as A-ions and Zr as B-ion in the eight compositional relations were prepared: Pb–Zr, (0.67Pb–0.33Ba)–Zr, (0.33Pb–0.67Ba)–Zr, Ba–Zr, (0.67Ba–0.33Sr)–Zr, (0.33Ba–0.67Sr)–Zr, Sr–Zr, and (0.33Pb–0.33Ba–0.33Sr)–Zr. These were repeated in each of the six rows of 8 in the 48 sample array. The corresponding product groups will be referred to as PZ-1, $(P_{2/3}B_{1/3})$Z-1, $(P_{1/3}B_{2/3})$Z-1, BZ-1, $(B_{2/3}S_{1/3})$Z-1, $(B_{1/3}S_{2/3})$Z-1, SZ-1 and $(P_{1/3}B_{1/3}S_{1/3})$Z-1, respectively, even if the real composition may deviate from the target composition. When individual samples are referred to, the cell reference will be added as, e.g. PZ-1 (A1). pH was varied by the addition of KOH to final concentrations of 1.0, 2.0 and 3.0 M KOH in pairs of rows. The resulting 24 compositions were prepared with and without a small amount of La (3% atomic relative to A-ions) in every second row, and the altogether 48 batches were crystallised at 200 °C for 6 h in the MultiAutoclave[4] (at autogeneous pressure). This time includes the time of heating up, which is about 1 h, before set temperature is reached.

In the second experimental series (series 2), A-ions Sr and La were excluded and another B-ion, Ti, and an additive, polyacrylamide (PAAm) was included. KOH concentrations of 2.0 M, 2.7 M, and 3.3 M were used. Two identical arrays with 48 batches in each were prepared, one was crystallised for 3 h and the other for 23 h at 200 °C, again including the heating up time of about 1 h. Eight different compositions on A- and B-ion reagent basis, Pb–Zr, (0.5Pb–0.5Ba)–Zr, Ba–Zr, Pb–Ti, (0.5Pb–0.5Ba)-Ti, Ba–Ti, Pb–(0.5Zr–0.5Ti), and Ba–(0.5Zr–0.5Ti) were prepared, with batch compositions as given in Table 1. The corresponding compositional product groups will in the following be referred to as PZ-2, $(P_{1/2}B_{1/2})$Z-2, BZ-2, PT-2, $(P_{1/2}B_{1/2})$T-2, BT-2, $P(Z_{1/2}T_{1/2})$-2, and $B(Z_{1/2}T_{1/2})$-2, respectively.

When necessary, "−2", and "/3 h" or "/23 h" will be added to distinguish samples of series 2 from series 1, and samples crystallised for 3 h and 23 h, respectively. Also, when addressing individual samples, the cell reference will be added as, e.g. PZ-2/23 h (A1).

After cooling, the solid products for the two series were transferred to a washing unit and washed five times with distilled water between cycles of centrifugation. The washed products were dried at 110 °C, and subsequently gently crushed before sample preparation for analysis.

2.2. Characterisation

Phase content analyses were based on powder X-ray-diffraction (XRD) data collected on a Bruker D8 Discovery diffractometer with Cu $K\alpha_{1,2}$-radiation. The diffractometer is equipped with Göbel mirror, general analysis diffraction detector system (GADDS), and an xyz-stage whereby 48 samples in one sample holder were analysed in each run. Each sample was run for 2 min covering the range 24–56° 2 theta in order to obtain an XRD-pattern of acceptable quality for phase identification. Scanning electron microscopy (SEM) analyses were run on a JEOL 5900LV equipped with an xyz-stage in the sample chamber. All samples were imaged in automated set-up screen-mode at a magnification of 2000×. At this magnification the autofocus and auto brightness functions could be used, but it was found advantageous to carry out manual adjustments on the first sample on each array. With this procedure, moving to, and imaging of one sample took about 2 min only.

Chemical analyses were done by wavelength dispersive spectroscopy (WDS) using a Cameca SX 100 microprobe, also equipped with a xyz-stage, allowing semi-automated operation. For "bulk" analysis, three 50 × 50 μm spots on each sample were analysed and averaged, with an uncertainty within ±2% relative. The penetration depth is 1–1.5 μm for the compositions analysed in the present work. The results were normalised to 100% for the sum of the six elements Ba,

Table 1
Reaction mixture and product compositions of the 23 h syntheses of [(Pb,Ba)(Zr,Ti)O_3] in series 2

	Reaction mixture composition (mmol/ml)						Product composition (at.%)					
	Pb	Ba	Zr	Ti	KOH	PAAm (wt.%)	Pb	Ba	Zr	Ti	K	Cl
A1	0.33		0.33		3.33	0.1	*32.3*		*63.2*		*3.4*	*1.0*
B1	0.33		0.33		3.33		*40.0*		*50.6*		*7.2*	*2.2*
C1	0.33		0.33		2.67	0.1	*37.5*		*55.6*		*4.3*	*2.6*
D1	0.33		0.33		2.67		*46.3*		*46.2*		*4.8*	*2.5*
E1	0.33		0.33		2.00	0.1	*59.1*		*29.1*		*8.3*	*3.3*
F1	0.33		0.33		2.00		44.7		45.6		5.7	3.8
A2	0.17	0.17	0.33		3.33	0.1	28.8	8.6	60.4		2.0	0.2
B2	0.17	0.17	0.33		3.33		28.9	5.1	65.1		0.9	0.1
C2	0.17	0.17	0.33		2.67	0.1	40.4	7.5	51.5		0.6	0.0
D2	0.17	0.17	0.33		2.67		33.0	4.9	61.7		0.4	0.0
E2	0.17	0.17	0.33		2.00	0.1	33.9	10.2	54.9		0.6	0.4
F2	0.17	0.17	0.33		2.00		35.4	9.9	54.4		0.3	0.0
A3		0.33	0.33		3.33	0.1		47.4	49.1		3.2	0.2
B3		0.33	0.33		3.33			49.9	49.0		1.0	0.1
C3		0.33	0.33		2.67	0.1		43.9	53.3		2.4	0.3
D3		0.33	0.33		2.67			47.2	51.2		1.4	0.2
E3		0.33	0.33		2.00	0.1		43.8	54.4		1.5	0.3
F3		0.33	0.33		2.00			37.9	59.9		1.5	0.6
A4	0.33			0.33	3.33	0.1	52.3			47.3	0.3	0.0
B4	0.33			0.33	3.33		53.3			46.5	0.2	0.0
C4	0.33			0.33	2.67	0.1	54.1			45.7	0.2	0.0
D4	0.33			0.33	2.67		53.6			46.3	0.1	0.0
E4	0.33			0.33	2.00	0.1	*46.7*			*37.0*	*1.9*	*14.3*
F4	0.33			0.33	2.00		*48.8*			*42.1*	*0.9*	*8.2*
A5	0.17	0.17		0.33	3.33	0.1	29.3	19.8		50.4	0.4	0.0
B5	0.17	0.17		0.33	3.33		30.5	19.2		50.1	0.1	0.0
C5	0.17	0.17		0.33	2.67	0.1	30.2	18.9		50.8	0.1	0.0
D5	0.17	0.17		0.33	2.67		30.3	19.1		50.4	0.1	0.0
E5	0.17	0.17		0.33	2.00	0.1	29.4	20.8		49.4	0.4	0.0
F5	0.17	0.17		0.33	2.00		*42.7*	*6.9*		*49.6*	*0.2*	*0.5*
A6		0.33		0.33	3.33	0.1		47.6		52.1	0.2	0.2
B6		0.33		0.33	3.33			47.2		52.2	0.1	0.2
C6		0.33		0.33	2.67	0.1		46.6		52.8	0.2	0.2
D6		0.33		0.33	2.67			48.5		50.8	0.2	0.3
E6		0.33		0.33	2.00	0.1		45.4		53.9	0.2	0.4
F6		0.33		0.33	2.00			45.8		53.8	0.1	0.3
A7	0.33		0.17	0.17	3.33	0.1	51.5		29.7	18.5	0.3	0.0
B7	0.33		0.17	0.17	3.33		51.8		28.2	19.7	0.3	0.0
C7	0.33		0.17	0.17	2.67	0.1	50.2		32.9	16.7	0.2	0.0
D7	0.33		0.17	0.17	2.67		56.0		21.4	22.4	0.2	0.0
E7	0.33		0.17	0.17	2.00	0.1	*43.7*		*18.6*	*18.3*	*9.3*	*10.1*
F7	0.33		0.17	0.17	2.00		50.2		26.0	23.8	0.1	0.0
A8		0.33	0.17	0.17	3.33	0.1		48.6	25.0	24.5	1.3	0.5
B8		0.33	0.17	0.17	3.33			46.6	27.8	24.1	1.0	0.4
C8		0.33	0.17	0.17	2.67	0.1		47.3	25.3	26.1	0.8	0.5
D8		0.33	0.17	0.17	2.67			47.9	24.1	26.4	1.0	0.5
E8		0.33	0.17	0.17	2.00	0.1		48.9	23.2	25.2	1.7	1.0
F8		0.33	0.17	0.17	2.00			44.3	26.7	26.3	1.8	1.0

Numbers given for samples that were amorphous, poorly crystalline, impure or containing other phases than perovskite are in italics. Product composition was determined by microprobe WDS analysis.

Pb, Zr, Ti, K and Cl. As standards, pure metals were used for Pb, Zr and Ti, $BaCO_3$ for Ba, a K-containing zeolite from Toyo Soda for K and NaCl for Cl.

A time saving procedure for rapid chemical- and morphology analyses was developed, in that both microprobe WDS and SEM analysis can be run on the same sample sets. Powders were pressed onto carbon tape spots on four 40 mm × 50 mm Al-plates with 12 samples on each. Carbon was first sputtered onto the samples before microprobe analysis, and then gold before performing SEM analysis.

3. Results and discussion

3.1. Effect of synthesis conditions on the formation of perovskite phases

Powder XRD patterns of the 48 products formed in series 1 [(Pb,Ba,Sr)ZrO_3] are shown in Fig. 1. It can be seen that with 3.0 M KOH (rows A and B) and 2.0 M KOH (rows C and D), with batch pH ≈ 14+ and 14, respectively, most mixtures containing Ba and Sr crystallised to fairly pure perovskites, whereas no traces of the perovskite phase could be detected in the samples crystallised in 1.0 M KOH (rows E and F) with batch pH between 4 and 5. These findings confirm that an elevated pH is normally required for these perovskite compositions to crystallise from salt solutions under hydrothermal conditions.[7,10] With the pure Pb-containing composition, only the 3.0 M KOH-sample without La (sample B1) produced perovskite, although impure and of poor crystallinity. Lanthanum had a very minor, negative effect on overall crystallinity, which can be seen by comparing row 1 with row 2 and row 3 with row 4 in Fig. 1. Apart from this, we have not studied the La containing samples in further detail.

Based on the findings described for series 1, the lower pH limit was raised in series 2 [(Pb,Ba)(Zr,Ti)O_3], A-ions Sr and La were excluded and another B-ion, Ti and an additive, PAAm was included (for details see Table 1). Powder XRD patterns for both the 3 h and the 23 h run in series 2 are shown in Fig. 2, with the upper set of XRD-patterns representing the 3 h product and the lower set the 23 h product for each composition. Comparing the XRD-patterns of the two runs it can be seen that degree of crystallisation varies with both composition and crystallisation time. The three groups of products prepared without Pb, namely BZ, BT and B($Z_{1/2}T_{1/2}$) constituted well crystalline perovskite phases already after 3 h. After 23 h most of the other compositions had also crystallised to pure or fairly pure perovskites. However, as in series 1, only one of the lead zirconate batches produced perovskite. This was the batch with 2.0 M KOH without PAAm, but also this product (F1 in Fig. 2) was of relatively poor crystallinity as compared to the other compositions. Cheng et al.[25] reported similar poor crystallinity for pure PZ in a series where other samples with as little as 20% Ti on B-ion position showed high crystallinity.

Based on the XRD-patterns, the series 1 and the 23 h-samples of series 2 have been divided into "pure perovskite" samples and "other" samples. The "pure perovskite" samples are those that are at least fairly crystalline and do not exhibit non-perovskite reflections of significant intensity. However, in order to have lead zirconate represented in this group, the less well-crystalline sample PZ-2/23 h (F1) has also been included. In the following, only these "pure perovskite" samples are referred to.

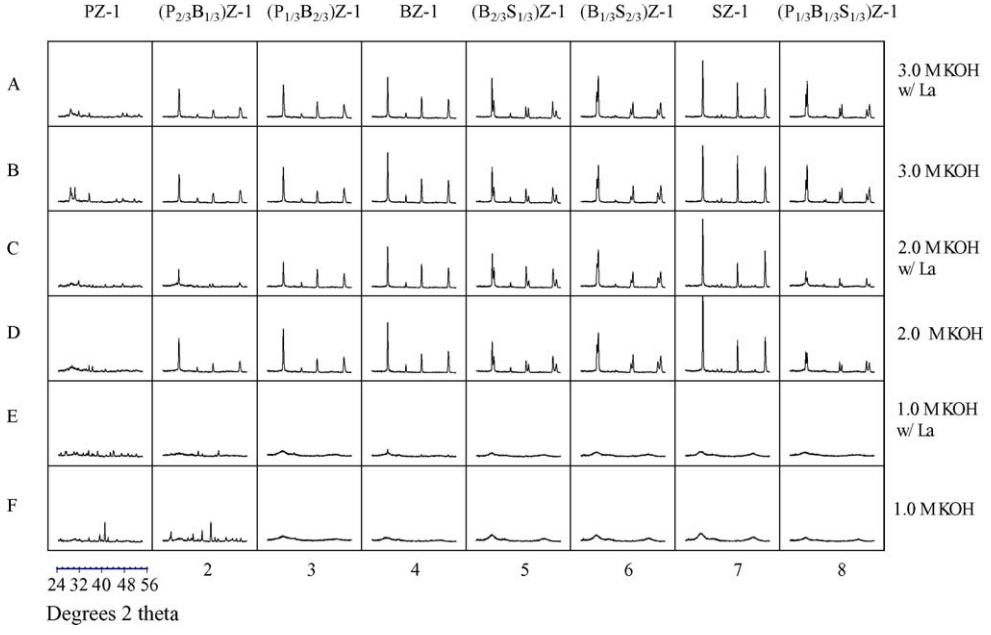

Fig. 1. Powder XRD-patterns (24–56° 2 theta) of experimental series 1 (Pb,Ba,Sr)ZrO_3. Crystallisation time was 6 h. Rows A and B: 3 M KOH. Rows C and D: 2 M KOH. Rows E and F: 1 M KOH. Small amount of La was added in rows A, C and E.

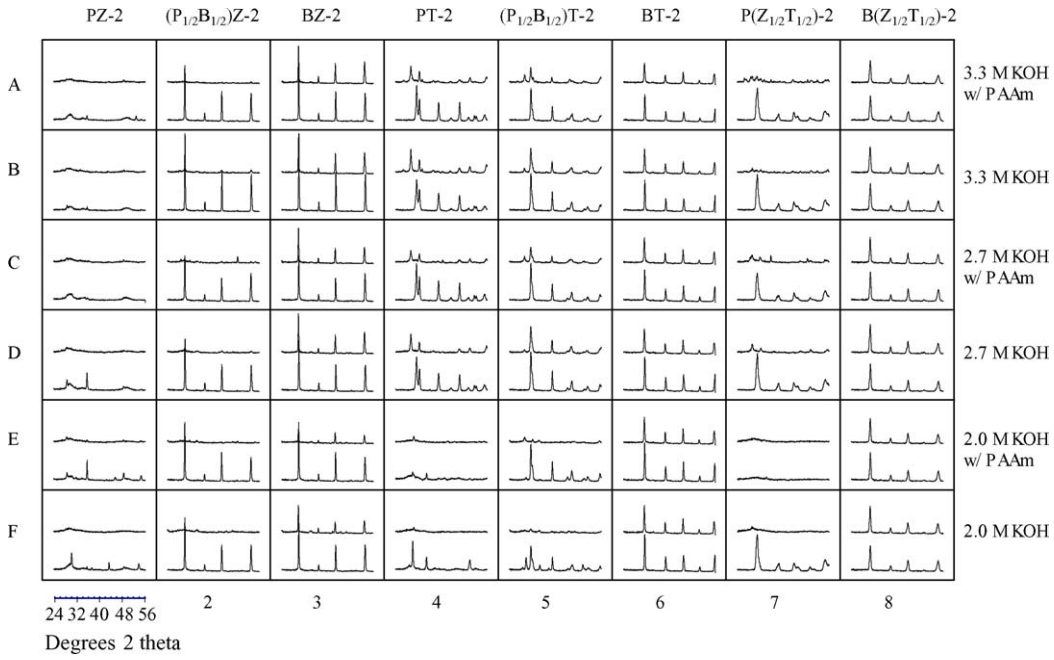

Fig. 2. Powder XRD patterns (24–56° 2 theta) of series 2. Upper XRD-pattern 3 h crystallisation time. Lower XRD-pattern 23 h crystallisation time. Rows A and B: 3.3 M KOH. Rows C and D: 2.7 M KOH. Rows E and F: 2 M KOH. PAAm was added in rows A, C and E.

For mixed compositions, it is of fundamental importance whether the different components crystallise as discrete phases or mixed phases. From Figs. 1 and 2 it appears that only the Sr-containing mixtures (columns 5, 6 and 8 in Fig. 1) seem to crystallise as two discrete phases, as judged from splitting in the XRD-reflections. A close-up of the reflections in the 29–33° 2 theta region (most intense peak for perovskites) of a set of samples from the BZ–SZ-compositional series is presented in Fig. 3. The position of the peaks and the observation that the ratio of the intensities of the two peaks closely reflect the batch compositions, (0.67Ba–0.33Sr)–Zr and (0.33Ba–0.67Sr)–Zr, respectively (Figs. 1 and 3), strongly indicates that BZ and SZ crystallise as two discrete phases, under the applied hydrothermal synthesis conditions. The other mixed compositions exhibit XRD-patterns with features in between those of the pure end member compositions (Figs. 4–7), indicating formation of mixed phases. The products $(P_{1/2}B_{1/2})$T-2 (Fig. 4) and the $P(Z_{1/2}T_{1/2})$-2 (Fig. 5) exhibit shoulders on the 30–32° 2 theta reflections whereas the reflection at about 45° is split (see Fig. 2), clearly indicating non-cubic symmetry, although less marked than for the tetragonal PT-phase which is an end member of both series (Figs. 4 and 5). According to Vold et al.,[9] a PBT with the same powder XRD-features as that in Fig. 4 is also tetragonal.

The PZT-system also represents a solid solution series between one cubic (or pseudocubic) and a tetragonal end member. Several groups have reported the coexistence of a tetragonal and a rhombohedral phase in PZT-samples containing about equal amounts of Zr and Ti.[16,22,25] It is however outside the scope of the present work to characterise the samples at this level of detail.

The peaks of the $(P_{1/2}B_{1/2})$Z-2 (Fig. 6) and $B(Z_{1/2}T_{1/2})$-2 (Fig. 7) are smooth without sign of splitting, and all the phases in the two series appear to be cubic (or pseudo-cubic), but both the $(P_{1/2}B_{1/2})$Z-2 and the $B(Z_{1/2}T_{1/2})$-2 have dis-

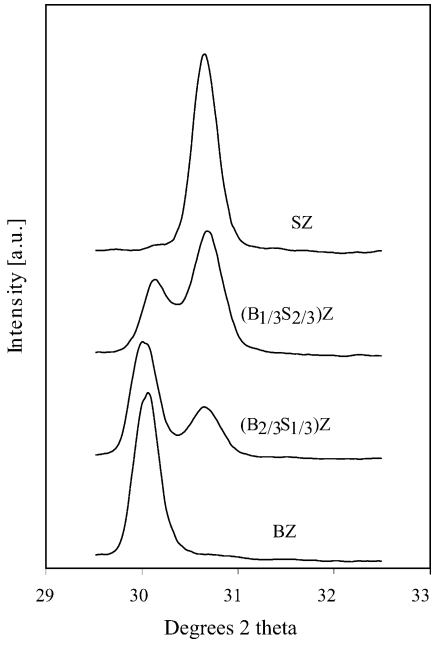

Fig. 3. Close-up of the 29–33° 2 theta-reflection from powder XRD patterns from series 1 of BZ (sample B4), $B(_{2/3}S_{1/3})Z$ (sample B5), $(B_{1/3}S_{2/3})Z$ (sample B6) and SZ (sample B7). The data have been smoothed.

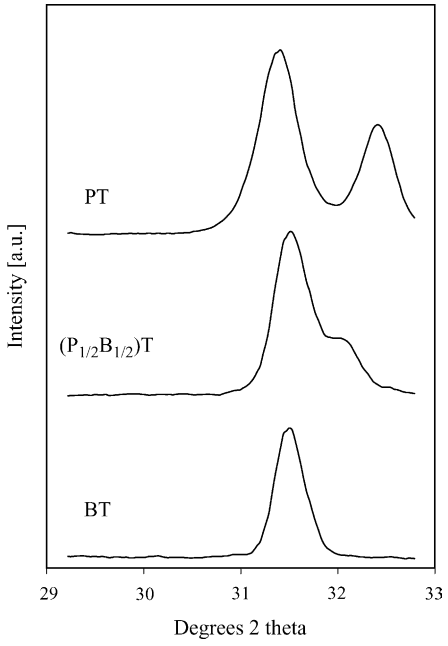

Fig. 4. Close-up of the 29–33° 2 theta-reflection from powder XRD patterns from series 2 (23 h) of PT (sample A4), $(P_{1/2}B_{1/2})T$ (A5) and BT (A6). The data have been smoothed.

tinctly broader peaks than the pure end members, and all the phases in the two series appear to be cubic (or pseudo-cubic). The thermodynamically stable form of BT for example is tetragonal at room temperature, but hydrothermally prepared samples often exhibit the metastable cubic symmetry,[9,11] in agreement with our findings. The observed peak broadening of the mixed phases will be discussed further below.

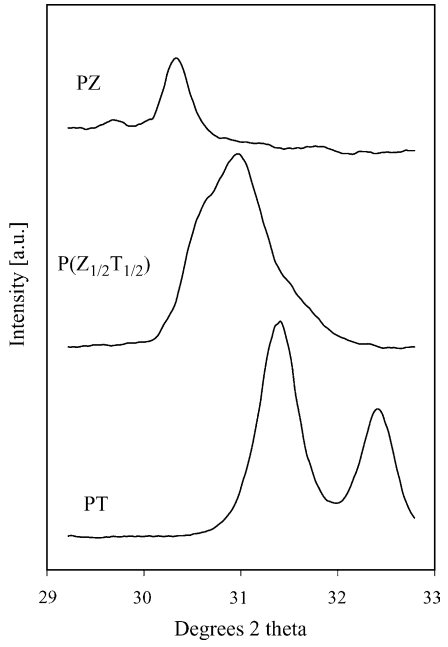

Fig. 5. Close-up of the 29–33° 2 theta-reflection from powder XRD patterns from series 2 (23 h), of PZ (sample F1), $P(Z_{1/2}T_{1/2})$ (A7) and PT (A4). The data have been smoothed.

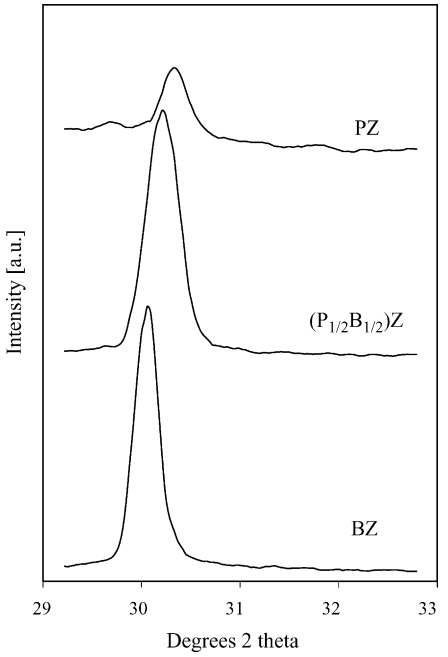

Fig. 6. Close-up of the 29–33° 2 theta-reflection from the powder XRD patterns of PZ (sample F1), $(P_{1/2}B_{1/2})Z$ (F2) and BZ (F3) from series 2 (23 h). The data have been smoothed.

3.2. Morphology — particle size and size distribution for series 2/23 h

SEM-micrographs of all the samples from series 2/23 h are shown in Fig. 8. Average particle size of each "pure perovskite" sample (see definition above) in series 2/23 h is

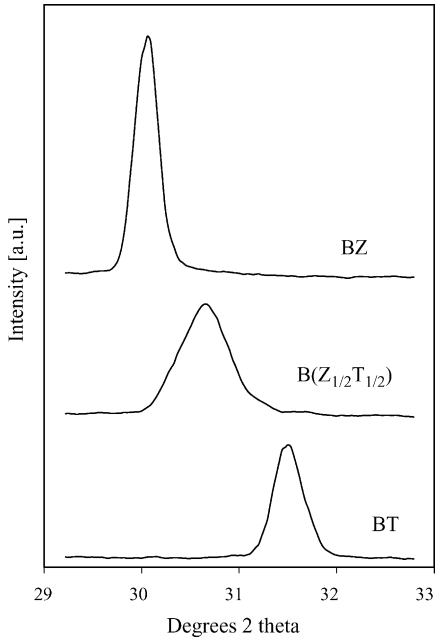

Fig. 7. Close-up of the 29–33° 2 theta-reflection from powder XRD patterns from series 2 (23 h) of BZ (sample A3), $B(Z_{1/2}T_{1/2})$ (A8) and BT (A6). The data have been smoothed.

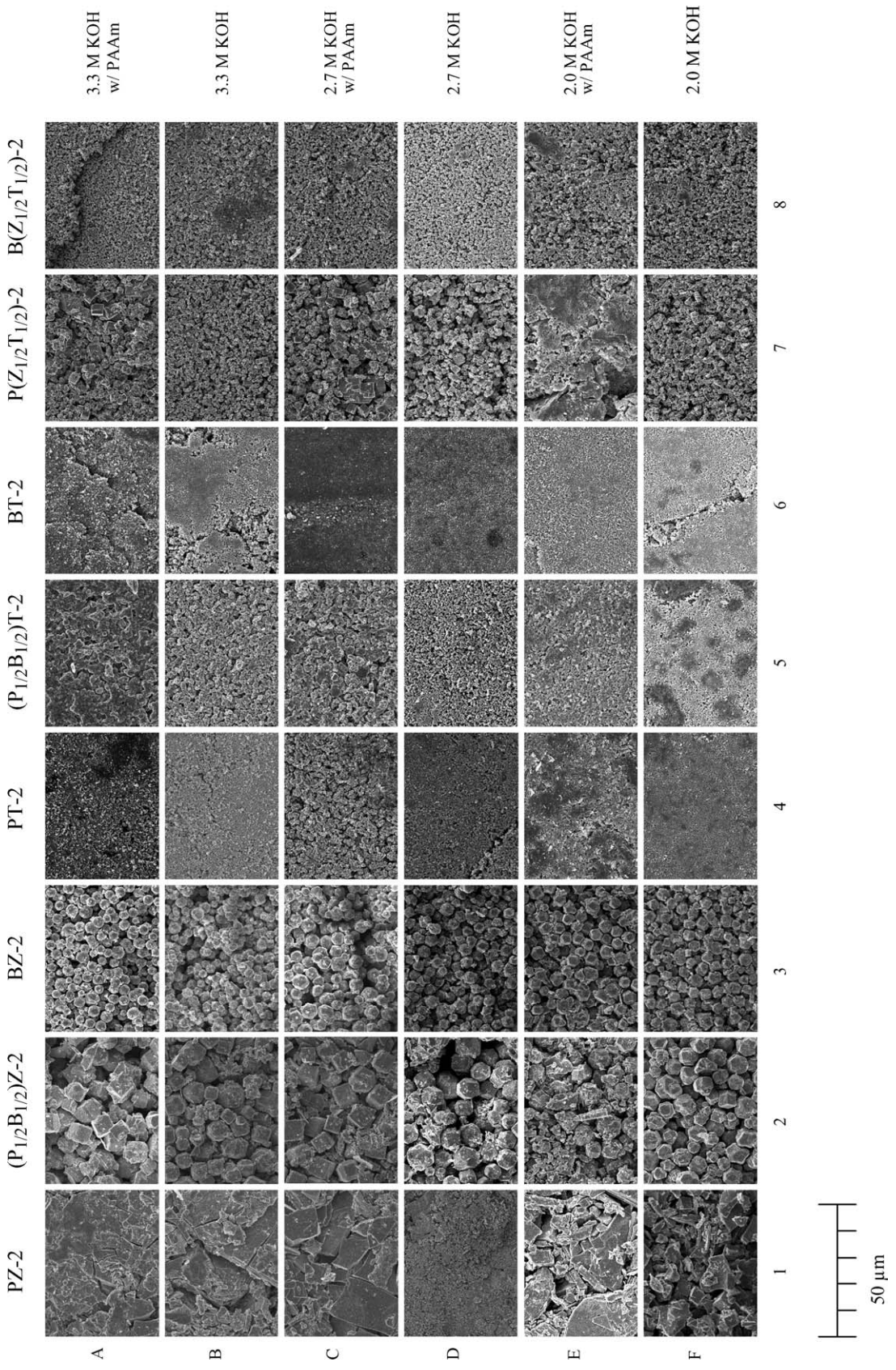

Fig. 8. SEM micrographs of the 48 samples of series 2 crystallised for 23 h. Original magnification 2000×.

Table 2
Approximate mean particle diameter (μm) as determined by measurement of clearly visible perovskite crystals in SEM-micrographs in Fig. 8

	PZ-2	PBZ-2	BZ-2	PT-2	PBT-2	BT-2	PZT-2	BZT-2	
A		7	3	0.3	0.7	0.3	0.8 + 4	0.5	3.3 M KOH w/PAAm
B		7	3	0.4	1	0.2	0.5 + 2	0.8	3.3 M KOH
C		8	4	0.7	1	0.4	1 + 5	0.9	2.7 M KOH w/PAAm
D		7	3	0.4	0.4	0.3	0.5 + 3	0.6	2.7 M KOH
E		6	4		0.6	0.4		0.7	2.0 M KOH w/PAAm
F	5	5	3			0.3	0.5 + 2	0.8	2.0 M KOH
	1	2	3	4	5	6	7	8	

Only the well crystalline (based on powder XRD) samples were analysed. For the samples with smaller particle size, 5000× magnification images were used. For the samples with larger particles, 2000×.

reported in Table 2. The particle size was estimated by visual inspection of the SEM-micrographs presented in Fig. 8. It must be stressed that from the micrographs, it was not possible to confirm or rule out if the particles are composed of agglomerates of monocrystals or not. In addition, the micrographs are not necessarily representative of the whole samples, so a precise determination based on these images could be misguiding, but trends can be deduced based on the more significant size differences observed. Firstly, the data show a high correlation between particle size and batch chemical composition in terms of A- and B-ions, but little effect of pH and PAAm-additive. There is a clear tendency for samples with Zr as the only B-cation to form large particles in the 3–8 μm-range whereas all samples containing Ti as only B-cation formed small particles, in the 0.3–1 μm-range. The rapidly crystallising products, namely BZ, $B(Z_{1/2}T_{1/2})$ and BT were made up of smaller particles than the corresponding slower crystallising compounds containing Pb (Fig. 8 and Table 2). $P(Z_{1/2}T_{1/2})$ is the only product composition that exhibits clearly bimodal particle size distributions, with a set of smaller particles in the 0.5–1 μm-range and a set of larger particles in the 2–5 μm-range (Fig. 9). For comparison, Fig. 10 shows a sample of the barium containing analogue $B(Z_{1/2}T_{1/2})$ made under the same conditions, which exhibits small, rather monodisperse particles.

The samples with PAAm-additive on average formed slightly larger particles than the corresponding samples without PAAm (Table 2 and Fig. 8). This was not expected, since Sato et al.[10] reported a positive effect of this additive for obtaining reduced particle size of $PbTiO_3$. However, the molecular weight of the PAAm used by Sato et al.[10] was not known, so the cause of the observed discrepancy cannot be assessed.

3.3. Chemical analysis of samples in the series 2/23 h

Product composition of the samples of series 2/23 h, as obtained from WDS microprobe analyses are given in Table 1, and the composition based on A- and B-ions is graphically shown as pie diagrams in Fig. 11. The samples which were not defined as "pure perovskite" are considered irrelevant and

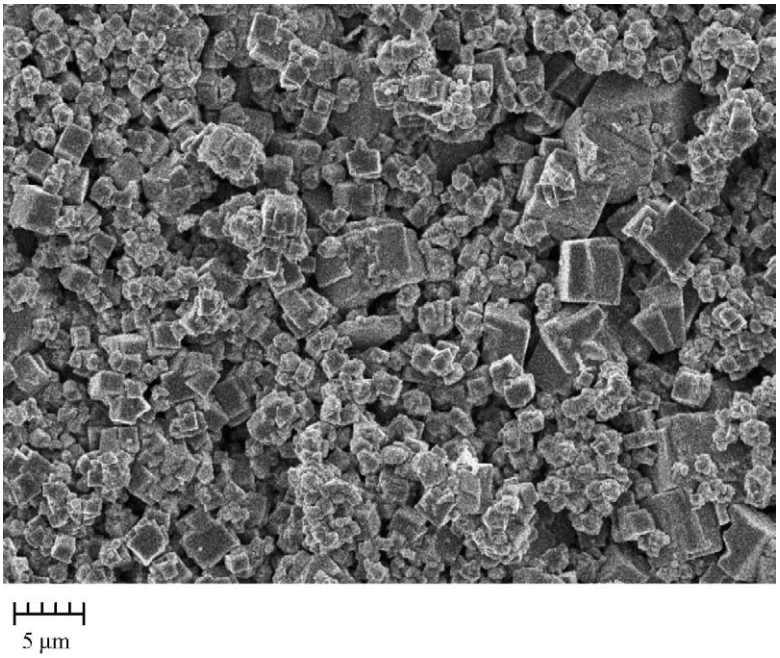

Fig. 9. SEM micrograph close-up of $P(Z_{1/2}T_{1/2})$ sample A7 from series 2 (23 h) in Fig. 8, showing particles of bimodal size distribution. Original magnification 2000×.

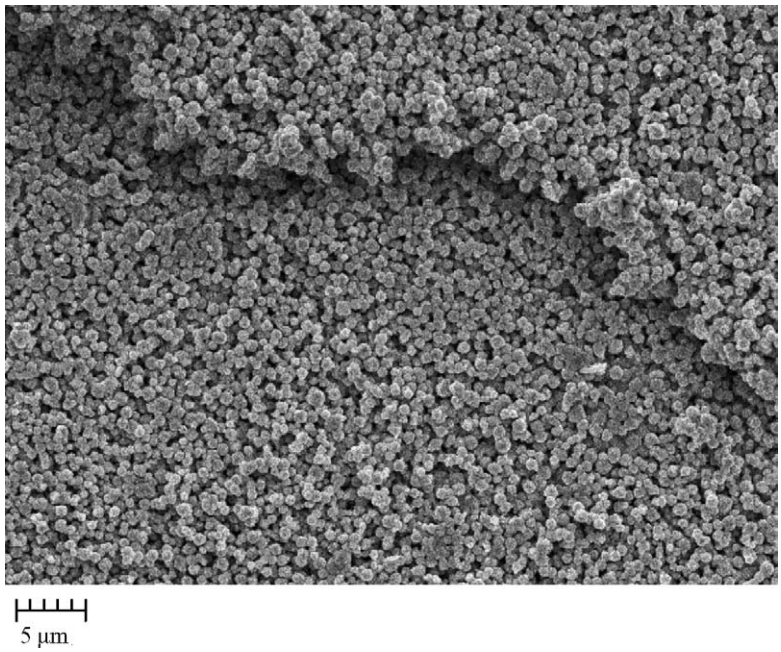

Fig. 10. SEM micrograph close-up of $B(Z_{1/2}T_{1/2})$ sample A8 from series 2 (23 h) in Fig. 8. Original magnification 2000×.

have been omitted in Fig. 11. The batch compositions of each column are shown in the upper row (marked R) of Fig. 11. The data presented in Fig. 11 and Table 1 show that, for the "pure perovskite" samples (as defined above) variation in KOH level and addition of PAAm had no clear effect on the chemical product composition.

The presence of potassium and chloride in the synthesis mixture represents a potential source of contamination in that K^+ can substitute for A-ions and Cl^- for oxygen.[20] The concentrations of these two ions in the 23 h samples are given in Table 1. The samples with the highest concentrations of potassium and chloride are generally the amorphous or poorly crystalline samples (italics in Table 1), all of which are lead-containing samples. However, some samples have 0.1% or less of potassium and chloride. Those are three of the $(P_{1/2}B_{1/2})T$ samples, one PT and one BT, all of which are well crystalline titanates with small particle size. There does not seem to be any correlation between KOH concentration in the reaction mixture and potassium-content in the well crystalline products. For chloride however, there is a trend that more chloride is included in samples prepared in lower KOH-concentration, even though the Cl^--concentration was the same in all reaction mixtures. Altogether, it is evident that certain compositions (in this case the titanates) can be crystallised in the presence of K^+ and Cl^-, with very little contamination of the crystalline perovskite products.

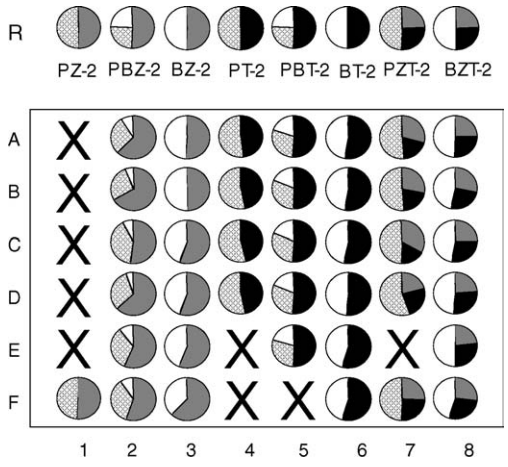

Fig. 11. Graphical visualisation of the chemical composition of the 48 products of series 2 crystallised for 23 h. Pb = grey grid, Ba = white, Zr = dark grey, and Ti = black. Upper row R represents synthesis mixture A- and B-ion composition for each of columns 1–8. Products that are not pure or fairly pure perovskites have been hatched out with an X.

The ideal perovskite structure would require a one-to-one balance between A- and B-ions. In this study we observed that for most samples the ratio between A- and B-ions deviates from 1, even taking account of K^+ as a possible framework substituent (Table 1). In most cases the deviation is beyond the level that can be explained by the analytical uncertainty, estimated to be in the range of ±2% relative. The observed discrepancies may well reflect the existence of non-perovskite compounds that are amorphous.

3.4. Correlating information from XRD, SEM and microprobe analyses

So far information obtained from the results of each of the applied characterisation techniques have been discussed separately. Further information may be extracted by correlating data from the three different methods.

Four of the compositional groups from series 2/23 h have compositions reasonably close to the synthesis mixture compositions (Fig. 11 and Table 1). Those are BZ, PT, BT and $B(Z_{1/2}T_{1/2})$, including the three compositions BZ, BT and $B(Z_{1/2}T_{1/2})$ that were fully crystalline already after 3 h. Thus, there appears to be a positive correlation between rate of crystallisation and preservation of the stoichiometry of the product with respect to the reagent mixture. Particle size (Fig. 8 and Table 2) however appears not to be correlated with crystallisation rate or stoichiometry, but only with chemical composition.

Turning now to the balance between Pb and Ba in the samples containing both these A-ions in series 2 (Fig. 11 and Table 1), both the zirconates and the titanates are apparently enriched in Pb relative to the synthesis mixture composition. However, since the microprobe analysis only represents a layer of 1–1.5 μm, less than half of the volume of the analysed $(P_{1/2}B_{1/2})Z$ particles is represented in the analyses, since these particles are in the 5–8 μm diameter range (Table 2). The $(P_{1/2}B_{1/2})T$ particles in contrast are in the 0.4–1 μm range, so for these samples the analyses should in this respect represent the bulk of the samples. The $(P_{1/2}B_{1/2})Z$-samples showed on the average a Pb/Ba-ratio of about 4, whereas in the $(P_{1/2}B_{1/2})T$-samples the Pb/Ba-ratio is about 1.5 (Table 1). Since the BZ-system crystallises more readily than PZ under the present conditions, one would not expect the mixed composition samples to contain four times more Pb than Ba. What one might expect is that BZ-rich crystals form first in a (0.5Pb–0.5Ba)–Zr-batch, subsequently becoming overgrown by successively Pb-richer layers. With such zoned crystal growth one would expect to observe broadening of the powder XRD-reflections, as actually observed for the composition in question (Figs. 4 and 6). Furthermore, if the crystallites of the mixed phases $(P_{1/2}B_{1/2})T$ and $(P_{1/2}B_{1/2})Z$ shown in the micrographs in Fig. 8 are monocrystals, their size is too large to contribute to peak broadening in the powder XRD patterns. The compositions under investigation possess pseudo cubic symmetry, supporting that in this specific case we can most likely assign the observed broadening to zoning.

In the samples with two B-ions, the Zr/Ti-ratio in the $P(Z_{1/2}T_{1/2})$-samples is about 1.5 whereas in the $B(_{1/2}T_{1/2})$ samples the Zr/Ti-ratio is around 1.0, the latter corresponding to the synthesis mixture composition. The $P(Z_{1/2}T_{1/2})$-samples are special in that they exhibit a bimodal particle distribution (Figs. 8 and 9 and Table 2) that might indicate a separation of phases, as previously discussed. The $B(Z_{1/2}T_{1/2})$-samples produced very small particles, so in this case the results can be regarded as reliably representing the bulk material. However, zoning may still be present due to the observed peak broadening in the powder XRD pattern.

4. Conclusions

It has been shown that combinatorial hydrothermal synthesis and characterisation techniques are fully applicable to the synthesis and basic characterisation of perovskites. With only a few selected series of experiments, the relation between several chemical composition variables, crystallisation rate and particle size was established for a multicomponent system. The power of the combinatorial approach is its potential for mapping of systems in multi-parameter space because a high number of experiments can be run in parallel for limited resources.

References

1. Briceno, G., Chang, H., Sun, X.-D., Schulz, P. G. and Xiang, X.-D., A class of cobalt oxide magnetoresistance materials discovered with combinatorial synthesis. *Science*, 1995, **270**, 273–275.
2. Reichenbach, H. M. and McGinn, P. J., Combinatorial solution synthesis and characterization of complex oxide catalyst powders based on the $LaMO_3$ system. *Appl. Catal. A: Gen.*, 2003, **244**, 101–114.
3. Akporiaye, D. E., Dahl, I. M., Karlsson, A. and Wendelbo, R., Combinatorial approach to the hydrothermal synthesis of zeolites. *Angew. Chem. Int. Ed.*, 1998, **37**(5), 609–611.
4. Wendelbo, R., Akporiaye, D. E., Karlsson, A. and Dahl, I. M., EP 0968050 B1, Assigned to Sinvent.
5. Akporiaye, D., Dahl, I. M., Karlsson, A., Plassen, M., Wendelbo, R., Bem, D. S., Broach, R. W., Lewis, G. J., Miller, M. and Moscoso, J., Combinatorial chemistry—the emperor's new clothes? *Micro. Meso. Mater.*, 2001, **48**, 367–373.
6. Holmgren, J., Bem, D. S., Bricker, M., Gillespie, R., Akporiaye, D., Dahl, I. M., Karlsson, A., Plassen, M. and Wendelbo, R., Application of combinatorial tools to the discovery and commercialisation of microporous solids: facts and fiction. In *13th International Zeolite Conference*, Montpellier, 2001. CD-ROM 03-K-01.
7. Dawson, W. J. and Swartz, S. L., 1992, US 5,112,433.
8. Lencka, M. M., Anderko, A. and Riman, R. E., Hydrothermal precipitation of lead zirconate titanate solid solutions; thermodynamic modeling and experimental synthesis. *J. Am. Ceram. Soc.*, 1995, **78**(10), 2609–2618.
9. Vold, R. E., Biederman, R., Rosetti Jr., G. A. and Sacco Jr., A., Hydrothermal synthesis of lead doped barium titanate. *J. Mater. Sci.*, 2001, **36**, 2019–2026.
10. Sato, S., Murakata, T., Yanagi, H., Miyasaka, F. and Iwaya, S. J., Hydrothermal synthesis of fine perovskite $PbTiO_3$ powders with a simple mode of size distribution. *J. Mater. Sci.*, 1994, **29**, 5657–5663.
11. Vivekanandan, R., Philip, S. and Kutty, T. R. N., Hydrothermal preparation of $Ba(Ti,Zr)O_3$ fine powders. *Mater. Res. Bull.*, 1986, **22**, 99–108.
12. Segal, D., Chemical synthesis of ceramic materials. *J. Mater. Chem.*, 1997, **7**(8), 1297–1305.
13. Lencka, M. M. and Riman, R. E., Thermodynamic modeling of hydrothermal synthesis of ceramic powders. *Chem. Mater.*, 1993, **5**(1), 61–70.
14. Zheng, W., Pang, W. and Meng, G., Hydrothermal synthesis of $SrZrO_{3-\alpha}$ (M = Al, Ga, In, $x \leq 0.20$) series oxides. *Solid State Ionics*, 1998, **108**, 37–41.
15. Moon, J., Suvaci, E., Morrone, A., Costantino, S. A. and Adair, J. H., Formation mechanisms and morphological changes during the hydrothermal synthesis of $BaTiO_3$ particles from a chemically modified, amorphous titanium (hydrous) oxide precursor. *J. Eur. Ceram. Soc.*, 2003, **23**, 2153–2161.
16. Lee, Y.-J. and Yen, F.-S., Phase-formation mechanism for hydrothermally synthesizing lanthanum-modified lead zirconate titanate powders. *J. Cryst. Growth*, 1997, **178**, 335–344.
17. McCormick, M. A. and Slamovich, E. B., Microstructure development and dielectric properties of hydrothermal $BaTiO_3$ thin films. *J. Eur. Ceram. Soc.*, 2003, **23**, 2143–2152.

18. Lencka, M. M. and Riman, R. E., Synthesis of lead titanate; thermodynamic modeling and experimental verification. *J. Am. Ceram. Soc.*, 1993, **76**(10), 2649–2659.
19. Cho, S.-B., Noh, J.-S., Lencka, M. M. and Riman, R. E., Low temperature hydrothermal synthesis and formation mechanisms of lead titanate ($PbTiO_3$) particles using tetramethylammonium hydroxide: thermodynamic modelling and experimental verification. *J. Eur. Ceram. Soc.*, 2003, **23**, 2323–2335.
20. Beal, K.C., Precipitation of lead zirconate titanate solid solutions under hydrothermal conditions. In *Advances in Ceramics: Ceramic Powder Science, Vol 21*, ed. G. L. Messing, K. S. Mazdiyasni, J. W. McCauley and R. A. Haber. American Ceramic Society, Westerville, OH, 1987, pp. 33–41.
21. Kutty, T. R. N. and Balachandran, R., Direct precipitation of lead zirconate titanate by the hydrothermal method. *Mater. Res. Bull.*, 1984, **19**, 1479–1488.
22. Traianidis, M., Courtois, C., Leriche, A. and Thierry, B., Hydrothermal synthesis of lead zirconium titanate (PZT) powders and their characteristics. *J. Eur. Ceram. Soc.*, 1999, **19**, 1023–1026.
23. Traianidis, M., Courtois, C. and Leriche, A., Mechanism of PZT crystallisation under hydrothermal conditions. Development of a new synthesis route. *J. Eur. Ceram. Soc.*, 2000, **20**, 2713–2720.
24. Piticescu, R. M., Moisin, A. M., Taloi, D., Badilita, V. and Soare, I., Hydrothermal synthesis of ultradisperse PZT powders for polar ceramics. *J. Eur. Ceram. Soc.*, 2004, **24**, 931–935.
25. Cheng, H., Ma, J., Zhu, B. and Cui, Y., Reaction mechanisms in the formation of lead zirconate titanate solid solutions under hydrothermal conditions. *J. Am. Ceram. Soc.*, 1993, **76**(3), 625–629.
26. Plassen, M., Automating a combinatorial hydrothermal synthesis and characterization with LabVIEW. *NIWeek 2001*. Austin, Texas, 2001. CD-ROM.